Solids backmixing and entrainment in the splash zone of large-scale fluidized bed boilers

(article starts on next page)

Solids backmixing and entrainment in the splash zone of large-scale fluidized bed boilers

Tove Djerf, David Pallarès *, Filip Johnsson

Division of Energy Technology; Department of Space, Earth and Environment; Chalmers University of Technology, 412 96 Göteborg, Sweden

ARTICLE INFO

ABSTRACT

This work studies the fluid dynamics of the solids in the splash zone of fluidized bed furnaces, with focus set on solids back-mixing and solids entrainment in order to enhance the understanding and prediction of the solids flow in the bottom region of the furnace. Experimental results show the establishment of a splash zone also for runs in absence of a dense bottom bed. A simple model assuming ballistic trajectories of the ejected solids is shown to satisfactorily estimate the solids back-mixing rate. The flux of non-backmixed solids, which are entrained from the bottom region, is found to be unaffected by the bottom wall configuration (tapered/vertical) for a given gas flow. Finally, an empirical expression is proposed for the solids entrainment from the bottom region which covers wide operational and unit size ranges.

1. Introduction

Fluidized bed (FB) combustion, which is a mature technology for heat and power production that has been commercialized for more than three decades, has as its main advantages inherent emissions control and fuel flexibility [1–3], which increase the possibilities to burn low-grade renewable fuels such as biomass waste from the forest industry. This gives the FB technology an important role in the phasing out of fossil fuels, which is needed to reach the targets set in the Paris Agreement [4]. A characteristic of circulating FB (CFB) boilers is the large solids inventory, which results in a thermal flywheel effect that yields relatively smooth temperature fields within the furnace. Thus, the solids flow plays a major role in both the mass and heat balances in the furnace, which are essential for the optimization, scale-up and development of the technology. Despite the FB technology being regarded as mature, there are still large knowledge gaps regarding the in-furnace processes, which result in uncertainties related to the prediction of the solids distribution in large-scale FB furnaces. The bottom part of the FB furnace consists of a dense bottom bed and a splash zone, and although these zones only occupy a small fraction of the furnace height (roughly 5%–10% of the furnace height), they contain the major share of the solids in the furnace [5]. In CFB boilers, the fluidization gas transports solids out of the bottom region and into the transport zone in the form of a dispersed phase (i.e., dominated by single-particle flow rather than clustered solids). This carryover of solids (herein termed *entrainment*)

from the bottom region into the transport zone is a key element in the performance of CFB furnaces, as it affects the extent of solids hold-up in the upper part of the furnace and, thereby, the heat transfer to the furnace walls and the flow of solids circulating externally through the cyclone. Furthermore, CFB furnaces often use tapered walls in the bottom region, in order to decrease the cross-sectional maldistribution of fuel and lateral gas injections and, supposedly, to increase the solids entrainment from the bottom region into the transport zone.

It is, therefore, important for the development of large-scale FB furnaces to understand the factors that govern the solids back-mixing in the bottom region, as this will determine the rate of solids entrainment into the transport zone. However, accurate experimental investigations of CFB units require a high spatial resolution for the measuring ports (typically, pressure taps); commercial CFB boilers have only a limited number of these ports. Nevertheless, there exist extensive measurements from the Chalmers 12-MW$_{th}$ CFB research boiler, based on which the fluid dynamics of the bottom bed and the splash zone have been characterized in greater detail [5–7]. Although the Chalmers boiler is operated under commercial conditions, its dimensions (1.42 × 1.62 × 13.5 m) mean that it is smaller than typical commercial CFB power boilers (with furnaces typically taller than 30 m). As a complement to experiments conducted at large scale, measurements carried out in cold models operating according to scaling laws can facilitate low-cost and highly flexible tests under conditions that quantitatively resemble those in large-scale boilers [8–13].

The aim of this work is to explore the fluid dynamics of the solids in the splash zone, so as to improve our understanding and ability to predict the solids backmixing in FB furnaces and the solids entrainment

---

* Corresponding author.
  E-mail address: david.pallares@chalmers.se (D. Pallarès).

Notation

a	decay coefficient of solids concentration in splash zone [1/m]
C_s	solids concentration [kg/m³]
$C_{s,\,entr}$	concentration of entrained solids from the bottom region [kg/m³]
d_p	particle size [m]
h	height from gas distributor [m]
H_b	dense bed height [m]
H_t	furnace height [m]
K	decay coefficient of solids concentration in transport zone [1/m]
L_x, L_y	boiler side dimensions [m]
u_g	fluidization velocity [m/s]
u_t	terminal velocity of single particle [m/s]
v_b	bubble rise velocity [m/s]
v_s	solids cluster ejection velocity [m/s]

Greek letters

ΔP_{ref}	bottom riser reference pressure drop (between 0.13 and 1.63 m) [Pa]
θ_{MAX}	maximal solids ejection angle [rad]
$\varnothing_h$	hydraulic diameter [m], $4L_x L_y/(2L_x + 2L_y)$
ξ	relative gas velocity [−] $\xi = u_g/u_t$
ρ_s	particle solid density [kg/m³]

Dimensionless numbers

Ar	Archimedes number, $\dfrac{g\,d_p^{\,3}\rho_g(\rho_s - \rho_g)}{\mu_g^2}$
d_p^*	dimensionless particle size, $d_p^* = Ar^{1/3}$
Re	Reynolds particle number, $\dfrac{\varnothing_h(u_g - u_t)\rho_g}{\mu_g}$
$G_{s,\,entr}^*$	dimensionless solids entrainment, $\dfrac{c_{s,entr}(u_g - u_t)}{\rho_s u_g}$
u^*	dimensionless gas velocity [−], $u^* = Re_p/Ar^{1/3}$

under circulating conditions. The objective is to identify the factors that govern the solids back-mixing in the splash zone, evaluate the accuracy levels of existing empirical correlations, and develop a general mechanistic description of the solids back-mixing. Additional objectives are to: (i) elucidate the parameters that govern the solids flux entrained into the transport zone and the possible effect that tapered walls have on this; and (ii) derive an expression that is capable of describing the solids entrainment for wide ranges of unit sizes, temperature levels, gas velocities and solids properties.

This work pertains to conditions relevant for commercial FB boilers, which are typically characterized by a furnace height to equivalent diameter aspect ratio ($H_t/\varnothing_h$) of <10, a dense bed to equivalent diameter aspect ratio ($H_b/\varnothing_h$) of <1, and solids in the Geldart group B [14,15].

2. Theory

Johnsson and Leckner [5] identified three different fluid-dynamical zones in the furnace of the Chalmers 12-MW$_{th}$ CFB boiler, which were subsequently confirmed in commercial-scale CFB furnaces [14,16,17] and studied in further detail in a fluid-dynamic down-scaled unit of a > 200-MW$_{th}$ CFB boiler [18]. These three fluid-dynamic zones are: (i) the dense bed, with a constant time-averaged solids concentration with height; (ii) the splash zone, with strong solids back-mixing that involves the ejection and back-mixing of solids clusters by means of a ballistic movement, yielding a fast exponential decay of the solids concentration with height; and (iii) the transport zone, where solids flow upwards as disperse particles in the core region and solids back-mixing occurs mainly at the furnace walls, yielding a weaker exponential decay of the average solids concentration with height [5]. Based on these observations, Johnsson and Leckner [5] have proposed an expression for the vertical profile of solids concentration above the dense bed (which is the differential solution of the flow development with height in the riser), and this has been developed further by the authors [19] to give:

$$C_s \rfloor_{h>H_b} = \left(C_s \rfloor_{h=H_b} - C_{s,entr}\right)e^{-a(h-H_b)} + C_{s,entr}e^{-K(h-H_b)} \tag{1}$$

where the solids entrained into the transport zone is expressed as a concentration, $C_{s,entr}$. The original expression described by Johnsson and Leckner instead used the solids concentration at the top of the riser [20], though that value results from a series of back-mixing phenomena and is, thus, more problematic to predict.

Fig. 1 shows a typical solids concentration profile from the Chalmers 12-MW$_{th}$ CFB boiler [5]. The logarithmic scale in the ordinate axis reveals the two above-mentioned exponential decays in the splash and transport zones, characterized by the constants a and K, respectively. The entrainment concentration is calculated through extrapolation of the transport zone profile down to the dense bed level (or down to the primary gas distributor if the dense bed is depleted), as indicated by the empty black circle in Fig. 1.
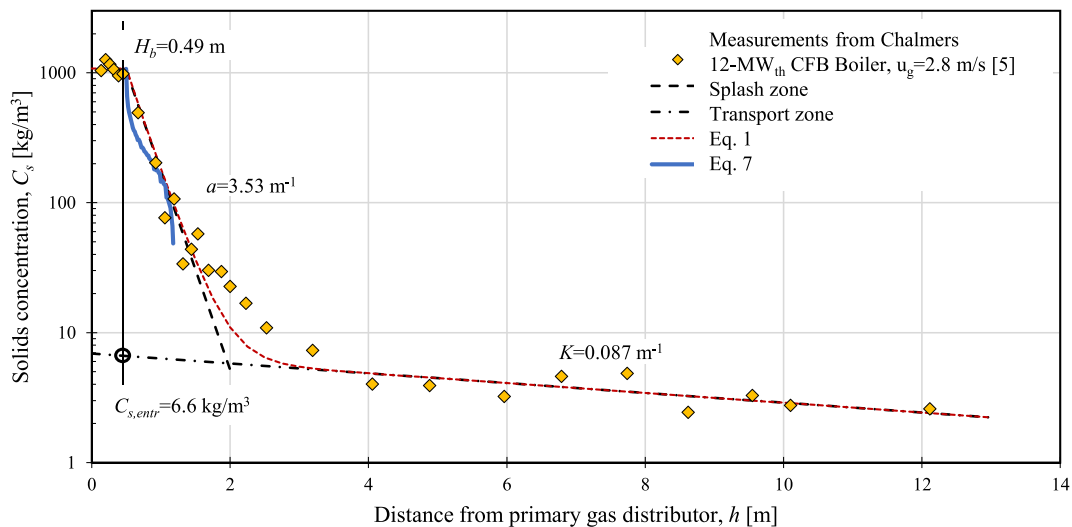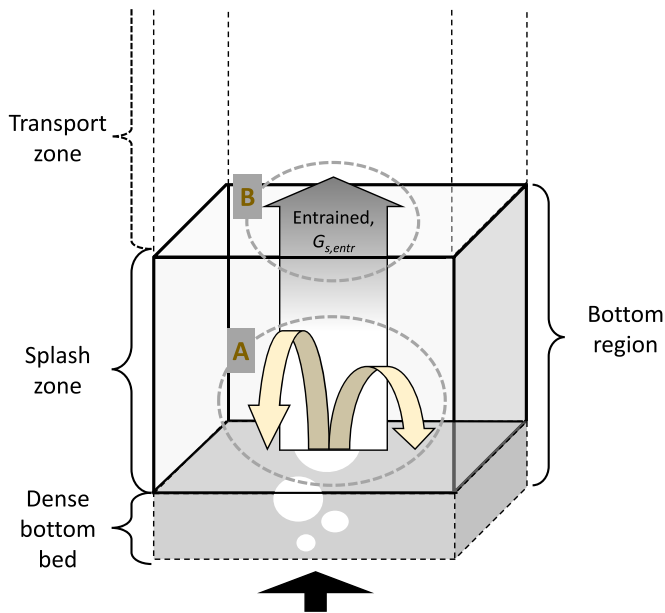

Fig. 1. Vertical profile of the solids concentration in the Chalmers 12-MW$_{th}$ CFB boiler [5], as: measured (markers), fitted to the semiempirical model by Johnsson and Leckner given by Eq. (1) (dashed lines), and – only for the splash zone – predicted using the ballistic model presented later in this work, Eq. (7) (solid line).

Fig. 2. Pathways for the solids mixing in the splash zone. A – solids back-mixing through cluster formation (described by the decay coefficient, a, in Eq. (1)), B – solids entrainment from the splash zone into the transport zone (described by the solids concentration, C_s,entr, in Eq. (1)).

The height of the dense bottom bed depends on the amount of solids (i.e., the riser pressure drop) and the fluidization velocity: with a given pressure drop, a sufficiently high fluidization velocity will eventually deplete the dense bottom bed (the region with constant vertical pressure gradient) and the particles will be redistributed along the height of the furnace [18,19,21,22]. The vertical distribution of solids in large-scale CFB furnaces in the absence of a dense bed has, however, not been studied in the literature. In this work, the experimental cases for which a dense bottom bed was detected are indicated by filled markers in plot figures, while cases without a dense bed are denoted by empty symbols. For the data in Fig. 1, the splash zone extends from the top of the dense bed (h = 0.49 m) up to a height of around 1.5 m above the gas distributor, with a decay in the solids concentrations from around 1000 kg/m³ to 30 kg/m³ represented by decay coefficient a in Eq. (1). The gas-solids flows of the dense bed and the splash zone are characterized by substantial fluctuations and, thus, the extension of the zones discussed above are such as those obtained from time-averaged values for the pressure drop. It should be noted that a dense bed is typically present (Fig. 1), despite the fact that the fluidization velocity exceeds the single-particle terminal velocity for the vast majority of the bed solids. This is attributed to the heterogeneous distribution of the gas flow in the dense bed, with the formation of a high through-flow within and in-between bubbles, typically in the form of a so-called *exploding bubble regime* [6,7]. When these void formations reach the dense bed surface an eruption occurs, and this ejects solids clusters into the splash zone [23,24]. During the ballistic trajectory of these solids clusters, some disperse particles attach and detach from the clusters and if detached, the particles are dragged upwards by the gas. In this situation, a flow of dispersed particles leaves the splash zone to enter the transport zone, as schematized in Fig. 2.

2.1. Solids ejection into the splash zone

Provided a large enough solids inventory (i.e. a high enough furnace pressure drop), large-scale CFB furnaces have been shown to hold a dense bottom bed, even when the fluidization velocity exceeds the terminal of the coarsest solids [6,18]. Such dense bed is similar to those

found in BFB boilers [6], with constant time-averaged solids concentration along its height and bubble volumetric fractions below 0.5 (i.e. a dense bed voidage less than approximately 0.75 [19,25] in contrast to the much higher voidages found in the bottom regions of narrow CFB units such as FCC cracker reactors). Further, there is typically no transition in pressure fluctuations with an increase in fluidization velocity in CFB boilers, i.e. pressure fluctuations do not exhibit a maximum but rather increase with velocity and then saturates at a certain value [26]. This behaviour is due to the typical characteristics of CFB boiler furnaces with group B solids, wide furnace geometries and a furnace pressure drop typically controlled at less than around 10 kPa [27]. Wang et al. (2021) have recently provided further studies of the flow regime in large-scale CFB boiler furnaces and referred to the regime as *bubbling-entrained bed* [28]. However, the bubble regime established in commercial CFB boilers differs from that formed in BFB units, reflecting the differences in the primary gas distributor. CFB gas distributors have lower pressure drops, to allow them to operate at higher velocity. The higher gas distributor pressure drop in BFB yields a finer bubble formation [6,7]. Bearing this in mind, the only visual studies on ejection of particles from the dense bed regard BFB units. In the presence of a dense bed, the ejection of solids clusters into the splash zone has been reported to be driven by the erupting gas voids [5,24], while the ejection mechanism in absence of a dense bed is not as well-studied. Based on experimental outcomes, Fung and Hamdullaphur [24] proposed an expression for the ejection velocity of the particle, which subsequently has been validated experimentally by Santana et al. [29]:

$$v_p = \left(1 - \frac{\theta}{\theta_{MAX}}\right) * 2 * v_b \rfloor_{h=H_b} * \cos(\theta) \qquad (2)$$

The bubble velocity as it reaches the dense bed surface can be calculated from different models described in the literature. Here, the set of expressions collected previously [14] is used. It combines the bubble growth model of Darton [30], bubble velocity described by Davidson et al. [31], the gas flow division reported by Johnsson et al. [9], and the through-flow share correlated from CFB boiler data [14]. Two aspects must be highlighted at this point in relation to the expressions used for bubble size and velocity. According to these expressions, the resulting ejection velocity increases with dense bed height, as taller beds foster larger gas bubbles, which in turn rise faster in the bed. Furthermore, for hot conditions, the Darton description of bubble growth sometimes yields erupting bubble sizes larger than the dense bed height – in these cases, the erupting bubble size is set as being equal to the height of the dense bed, according to the experimental findings in [6]. It should be noted that the Darton expression for bubble growth is directly applicable to beds with Geldart Group A and B solids in which bubble splitting is not dominant, but not for beds with a significant amount of group C or D solids [32]. For the latter, once the minimum fluidization velocity is exceeded large spherical bubbles which quickly coalesce into large spouting or slugging gas pockets. Even if mixtures of group B and D solids are able to yield an apparently more classical bubble flow, such beds are found to behave in a less periodic manner and more random bubble motions, with relatively small influence of the fluidization velocity [33]. Further, the complexity of the flow in beds consisting of D solids is increased by the fact that initial conditions can play a key role in the characteristics of the flow dynamics established [34]. For the velocities typically employed in CFB boilers, the bubbles will be of an exploding type, stretching all the way from the gas distributor to the top of the bed, causing a high through-flow of the gas [6].

2.2. Solids back-mixing – solids decay coefficient in the splash zone

The decay coefficient, a [see Eq. (1) and Fig. 1], has been studied experimentally in the fluidized bed literature. Kunni and Levenspiel [35] shows that laboratory scale CFB unit follows:

$$au_g \approx constant \tag{3}$$

However, very few experimental values obtained under conditions representative of large-scale CFB boilers (wide geometries, Geldart group B solids and relatively high fluidization velocity) are available, due to the requirement of a high spatial resolution in the solids concentration profile. Based on the data from runs carried out with three different particle sizes in the Chalmers 12-MW$_{th}$ CFB boiler, Johnsson and Leckner [5] have proposed the following, which includes the single particle terminal velocity (given the lack of information on the cluster size):

$$a = 4\frac{u_t}{u_g} \qquad H_b = 0.34 - 0.64m \tag{4}$$

Values of the decay coefficient in the splash zone representative of large-scale CFB combustors were also reported from experiments conducted in the fluid-dynamically down-scaled model of a commercial unit presented previously [18]. However, they were not analyzed further. Recent studies have shown that, in a unit run under cold conditions, the solids back-mixing in the splash zone decreases as the dense bed height is increased [19].

2.3. Entrainment of solids from the splash zone into the transport zone

The literature on fluidized beds contains numerous studies on the entrainment of particles: However, caution must be exercised in relation to the different meanings proposed for the concept of "entrainment" in the different works, depending on the type of unit or application. For BFB units (for example, see [36]), there is no significant solids entrainment above the splash zone, and solids entrainment typically relates to the flow of cluster solids ejected from the dense bed surface into the splash zone. In contrast, in narrow CFB units such as FCC reactors (for example, see [37]), entrainment typically refers to the solids leaving the riser and, thus, externally circulating the system through the return leg. In this study of large-scale CFB furnaces, the solids entrainment from the bottom region is in focus and is defined as the flux of particles leaving the bottom region (i.e., the conjunction of the dense bed and splash zone) and thereby entering the transport zone (Pathway B in Fig. 2). Note, however, that for the sake of simplicity in the analysis of the experimental data and for alignment with Eq. (1) (used in the mathematical models), the value used to characterize this entrainment, $C_{s,entr}$, is expressed in terms of a concentration of disperse solids at the dense bed surface. As disperse solids are assumed to flow according to their single-particle terminal velocities, the flux of dispersed solids assumed to be entrained from the time-averaged location of the dense bed surface is expressed as:

$$G_{s,entr} = C_{s,entr}(u_g - u_t) \tag{5}$$

Literature contains several works reporting solids concentration profiles in large-scale CFB boilers e.g. [38–40]. Yet, only a few works [36,41,42] have studied the entrainment of solids flow in relatively wide risers. To the best of our knowledge, studies in the literature on solids entrainment from the bottom region of large-scale CFB boilers are limited to recent work that the authors carried out under three different experimental conditions [18,19,22]: a pseudo-2D unit, a 3-D cold unit, and a 3-D fluid-dynamically down-scaled model. These works show that the entrained solids concentration increases with fluidization velocity, with no influence of the dense bed height as long as a dense bed is maintained, while the entrained solids concentration remains constant with an increase in fluidization velocity once the dense bed is depleted. Furthermore, injections of gas from the furnace walls (such as secondary air or recirculated flue gas) have been shown to strongly influence the entrained concentration of solids, increasing it if injected into the dense bed and decreasing it otherwise.

Finally, it should be noted that it is possible to generalize the entrained solids flux by expressing it in terms of a dimensionless solids flux, as derived in fluid-dynamic scaling studies (for example [13,43]):

$$G^*_{s,entr} = \frac{G_{s,entr}}{\rho_s u_g} \tag{6}$$

3. Method

This work combines analyses of experimental data (both from the literature and original findings from the present work), literature correlations and original mathematical modeling. Measurements are used to examine the ejection of the solids into the splash zone under different conditions, to evaluate the validity of literature expressions for the decay coefficient, and to propose a correlation for the entrained concentration of solids. The rate at which solids back-mixing in the splash zone occurs is modeled by means of a Monte Carlo simulation, so as to evaluate whether it can be mathematically described through ballistic trajectories.

3.1. Experimental work

The sources for the experimental data used in this work are listed in Tables 1 and 2 and cover a wide range of furnace sizes and solids properties (though all belonging to Geldart group B) and includes runs conducted under both hot and cold conditions. In summary, the measurement data used have been sampled in three different CFB units: the Chalmers 12-MW$_{th}$ CFB boiler [44]; a 3D cold unit operated under ambient conditions and both with and without (measurements in this work) fluid-dynamically scaled solids [18] (if scaling is used, it resembles hot operation in an existing >200-MW$_{th}$ CFB boiler, see [18]); and a pseudo-2D unit under ambient conditions [22]. Not all the datasets are used in the analyses of all the phenomena reported in the results section, but we have taken into account the suitability of the experimental conditions (e.g., owing to its geometry, the pseudo-2D unit would not provide with quantitatively relevant data for the solids entrainment) and the limitations linked to the data itself (e.g., direct comparison between a regular and a tapered bottom geometry could only be carried out with data from the scale model). See Tables 1 and 2 for the various setups used in this work.

3.2. Monte Carlo modelling of solids trajectories

The Monte Carlo modelling principle is employed to evaluate whether the ballistic trajectories of the ejected solids up in the splash zone can describe (both qualitatively and quantitatively) the exponential decay in solids concentration observed experimentally in the splash zone. Given an initial velocity for the ejected solids in the vertical direction, v_s, these are assumed to follow a ballistic trajectory that yields a vertical location dependent upon time, according to:

$$y(t) = v_s t - \frac{gt^2}{2} \tag{7}$$

Note the strong simplification inherent to disregarding the gas drag on the solids clusters, i.e., gravitation is the only force considered. This simplification is grounded on the fact that the splash zone of CFB boilers is dominated by solids clusters rather than dispersed solids as is the case in the transport zone (cf. Eq. (1) and [5]). In contrast to single particles, the gravity force of the solids clusters dominate over the gas drag as a consequence of their large size (and thereby they typically follow a ballistic movement, as reported in literature from visual observations [22]). Note that neglecting the gas drag on the ejected clusters removes the need for determining or modelling the cluster size when formulating the description for cluster trajectories given by Eq. (7). The initial condition of ejection velocity is calculated according to the model proposed by Fung and Hamdullaphur [24], which considers the bubble velocity

Table 1
Experimental data used in this work.

Unit		Size ($L_x \times L_y \times H_t$) [m]	Fluidization velocity, [m/s]	Riser pressure drop, [kPa]	Dense bed height, [m]	Temperature level, °C	Reference
Chalmers 12-MW$_{th}$ CFB boiler		$1.4 \times 1.6 \times 13$	1.1–6.3	6.0–7.5	0–0.64	850	Unit description in [44] Measurements in [5–7]
3D cold unit	Non-scaled material	0.445 m^2 × 3 m	0–1.4	0–3.5	0–0.26	25	Unit description in [19] Measurements this work
	Scaled material	75 m^2 × 40 m	0.5–4.5	3.2–8.4	0–1.2	850 *(after up-scaling)*	Unit description in [18] Measurements in this work and [18]
Pseudo-2D unit		$0.7 \times 0.12 \times 8.5$	0.3–7.0	2.8–10.2	0–0.58	25	Unit description in [22] Measurements in this work and [7]

[see Section 2.1 and, more specifically, Eq. (2)]. A time step of $2 \cdot 10^{-3}$ s is used for the time discretization of the axial trajectories of the clusters governed by Eq. (7), and the vertical locations at each time step are assigned to bins with a vertical size of 0.02 m, thus building up a probability density function profile for the axial concentration of the solids clusters. The decay constant for this probability density profile can be derived and compared to experimental values. Further, the probability density profile can be transformed into a concentration profile by setting the solids concentration at the bottom equal to the one measured in the dense bed (see e.g. Fig. 1). A numerical study showed that simulating in the order of 10^4 trajectories ensured robustness of the statistics obtained. For each trajectory simulated, the time-tracking is stopped when the solids have fallen back to the height from which they were ejected in Fig. 1, the solids concentration profile that results from the modeling with a simulation of the Chalmers 12-MW$_{th}$ boiler is plotted as a blue line. It is clear that the vertical profile of the solids concentration obtained from the model fits reasonably well to an exponential curve, and that the exponential constant from the simulated profile ($a = 2.97$ m^{-1}) is in good agreement with the experimental value ($a = 3.53$ m^{-1}). Note that this simple model provides a reasonable description for the lower part of the splash zone only, i.e., the region in which the gas drag is of less relevance and the solids flow is driven by inertia and gravity (which corresponds to the model assumption). Thus, the model must be considered as a tool for the determination of the decay coefficient value rather than a description of the solids concentration across the whole splash zone.

4. Results and discussion

4.1. Solids back-mixing – solids decay coefficient in the splash zone

The left-hand-side plots in Fig. 3 show the solids concentration decay coefficient as a function of the relative gas velocity (defined as $\xi = u_g/u_t$) for the different experimental setups listed in Tables 1 and.

Table 2. Thus, for these plots, values of the x-axis larger than 1 indicate a region with significant solids entrainment and circulation. The right-hand-side of Fig. 3 plots the decay coefficient as a function of the dense bed height for data series grouped according to the relative gas velocity ξ. The measurements from the two cold units (Fig. 3, a–f) include data series sampled at different riser pressure drops (which give a rough indication of the mass loading and different dense bed heights), while the measurements from the Chalmers boiler (Fig. 3, g–h) were carried out with similar dense bed heights ($\Delta p_{0-1.6m} = 7$ kPa; see [5]) but for three different average bed particle sizes. Furthermore, the empirical correlation for the splash zone decay coefficient expressed by Eq. (4) is added to these plots for comparison.

The dependency of the decay coefficient on the relative gas velocity (earlier reported in [5] based on the data shown in Fig. 3g) is observed to hold as a general trend for panels a, c, and e in Fig. 3 (albeit not as pronounced as in Fig. 3g). As seen from Fig. 3, the agreement of literature correlations for the decay coefficient to measurement data is generally poor (obviously, the correlation in Eq. (4) derived through data from the 12 MW unit fits these particular data points well). This reveals the need for a general formulation providing values of the decay coefficient which agree with the different sets of experimental data available in literature. The dependency on the dense bed height reported in [19] (higher dense bed yields lower decay coefficient) is not seen to hold as a general trend. Only data sampled in the pseudo-2D unit (Fig. 3b) show a stable dependency on bed height for the decay coefficient. Indeed, complementing with new measurements the data originally presented for the 3D cold unit [19] reveals (Fig. 4d) that the decay coefficient is relatively independent of the bed height, as long as there is sufficient height. However, when the dense bed is close to disappearing, the value of the decay coefficient increases. Thus, increasing the fluidization velocity decreases the decay coefficient, and the dense bed height is seen to affect the value of the decay coefficient only for the pseudo-2D unit, and not for the 3D units. This difference between the splash zones established in pseudo-2D and 3D units is investigated below in terms of the erupting bubble size (a key parameter, since the splash zone is considered to be populated by solids ejected from bubble eruptions at the dense bed surface).

The standard deviation of the in-bed pressure fluctuations is known to correlate to the bubble size, i.e., the larger the bubble size the greater the amplitude of the fluctuations. Fig. 4 displays pressure fluctuation data from cases in which a dense bed has been identified, showing that the standard deviation of the pressure fluctuations (i.e., the erupting bubble size) measured in the bottom region of the pseudo-2D unit increases with increasing bed height [6,7]. However, for the Chalmers CFB boiler, it seems to stabilize for typical dense bed heights >0.4 m. This suggests that the bubble size yields an equilibrium size, and does not grow further even if the dense bed height would allow it. This limitation on bubble growth with height in 3D units contrasts with the larger bubbles in the pseudo-2D unit, for typical intervals of the bed height, and is a suitable explanation for the variable trends

Table 2
Materials and experimental setups used in this work for the study of: i) the solids back-mixing described by the decay coefficient, a (first four rows), and ii) the solids entrainment from the bottom region into the transport zone described by the solids concentration, $C_{s,entr}$ (last five rows). Numbers in parentheses correspond to the values in cold flow models scaled to large-scaled hot conditions.

Unit	Particle material	Particle density ρ_s [kg/m^3]	Particle size d_p [µm]	Bottom sidewalls configuration
Pseudo-2D unit	Glass	2600	316	Vertical
3D cold unit	Glass	2600	211	Vertical
3D scale unit	Copper	8920	35 (*194*)	Vertical
Chalmers 12-MW$_{th}$ CFB boiler [5]	Sand	2600	200, 320, 440	Vertical
3D scale unit	Copper	8920 (*2470*)	35 (*194*)	Tapered
3D cold unit	Alumina	3950	122	Tapered
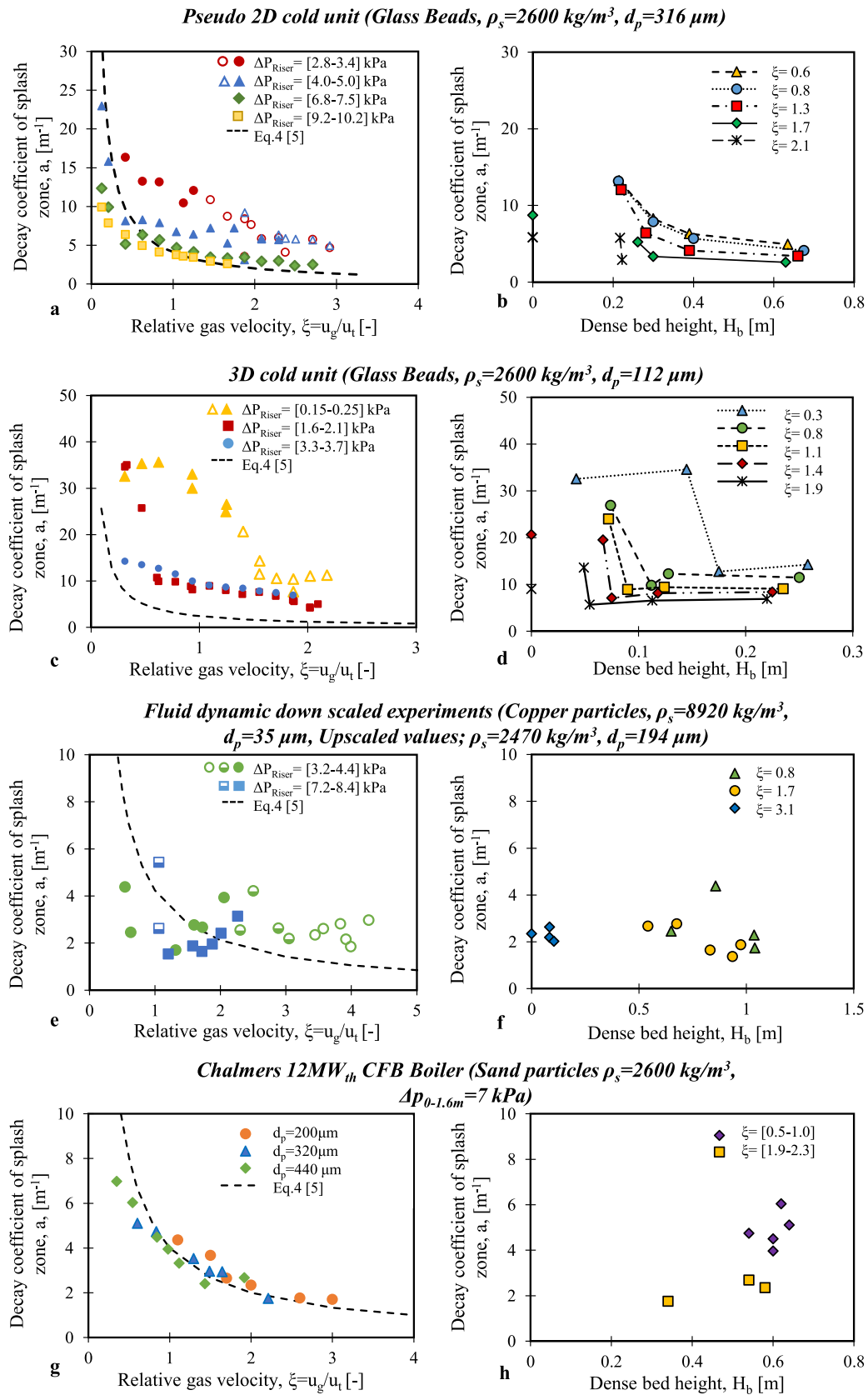
Fig. 3. Decay coefficient, a, as a function of the relative gas velocity, $\xi = u_g/u_t$ (left-hand plots) and of the dense bed height (right-hand plots); for the three different experimental set-ups: a-b) pseudo-2D unit; c-d) 3D cold unit; e-f) scale model of >200-MW$_{th}$ CFB boiler; g-h) Chalmers 12-MW$_{th}$ CFB boiler [5]. Plots a, c and e show the data series grouped according to pressure drop across the riser, and plot g shows the data series grouped according to particle size.
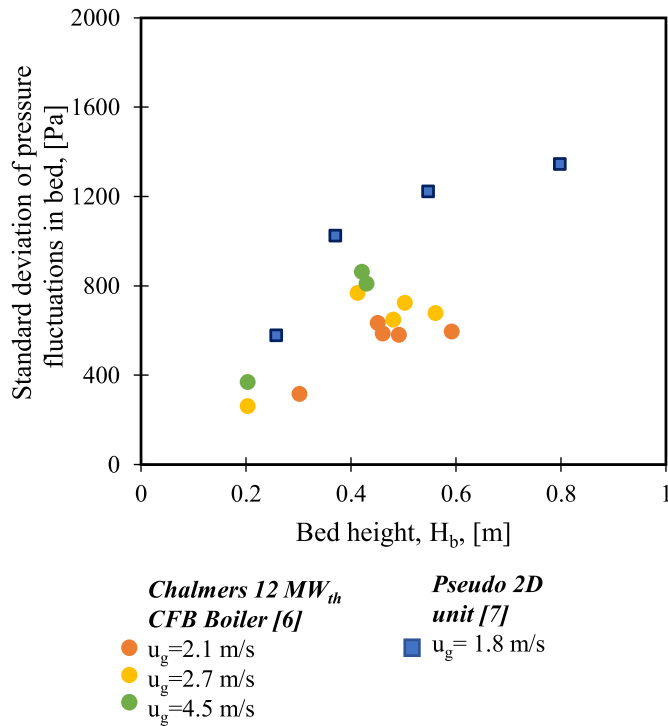
Fig. 4. Standard deviation of the pressure fluctuations in the dense bed (indicating the erupting bubble size) as a function of dense bed height. Data measured in the Chalmers boiler [6] and the pseudo-2D unit [7].

around 0.4 m, the pressure fluctuations increase with fluidization velocity initially (from 2.1 to 2.7 m/s) but exhibit saturation to this maximum for further increase (to 4.5 m/s) – in contrast to the typical transitional behavior to fast and turbulent fluidization obtained in narrow units with group A solids [35]. Notice that in the figure, for a given dense bed height the pressure fluctuations are stronger in the pseudo-2D unit than in the boiler despite the higher fluidization velocity in the latter. This can be explained through the different properties of the bubble flow established in pseudo-2D and 3D units [45]. In this sense, while the pseudo-2D unit has a limited depth of 0.12 m, its width (0.7 m) is visually confirmed to be large enough to allow bubbles to grow freely (without originating slugging) in this other lateral dimension as they rise along the dense bed height. Further, another reason for this experimental observation of more limited bubble growth in the 12 MW boiler could be the fact that bed material in this unit contains a larger share of group A fines (from long-term attrition of ash and char) that are known to enhance bubble split and thereby impede bubble growth.

As shown in Fig. 3, the empirical correlation for the decay coefficient proposed in literature on the basis of experiments conducted in the Chalmers CFB boiler [Eq. (4)] describes with significantly lower accuracy the decay coefficient under hot, large-scale conditions up-scaled from experiments in the 3D cold unit (Fig. 3e). Furthermore, the referred empirical correlation does not account for the dense bed height and is, therefore, unable to reproduce with good accuracy the experimental values derived from the experimental setups where the dense bed height affects the resulting solids back-mixing (i.e., the pseudo-2D and, possibly, the cold 3D experiments). As an alternative, the prediction of the decay coefficient through the model presented in Section 3.2 is assessed in Fig. 5, which shows the experimental values for the decay coefficient that are representative of hot, large-scale conditions and the corresponding values modeled according to Section 3.2 [Eq. (7)] and correlated [Eq. (4)]. Since the model presented in this work is based on the ejection of bed material into the splash zone from bursting bubbles in the dense bed, data in Fig. 5 includes only cases in which a dense bed was experimentally identified. As presented, the empirical correlation exhibits a better fit than the model to the experimental data from the Chalmers boiler, since this was the dataset to which it was fitted. The model still shows reasonable agreement with
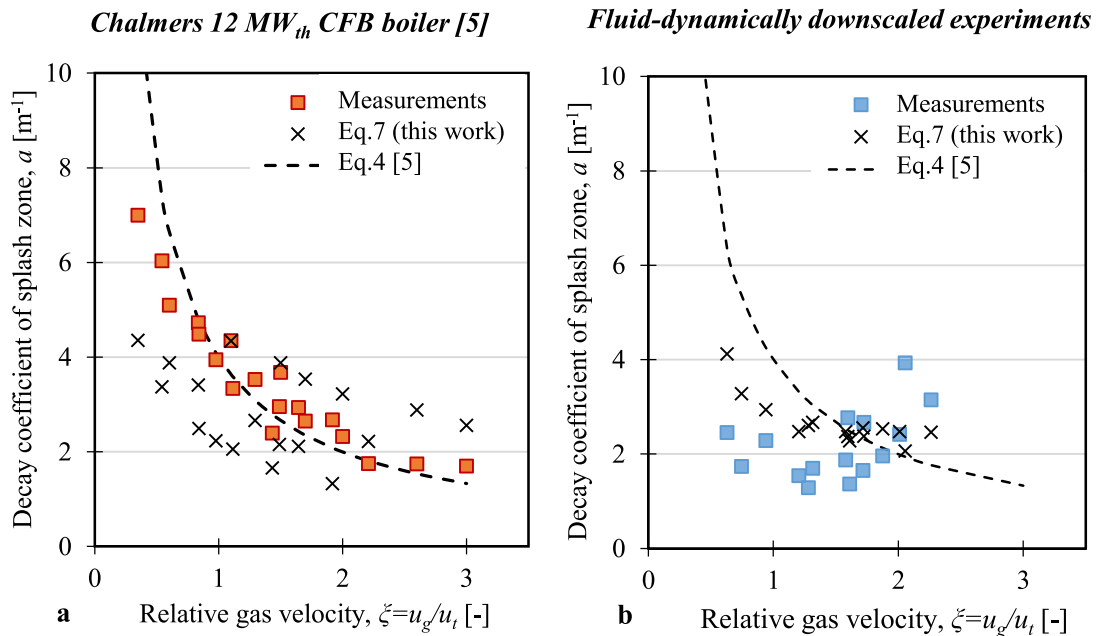
observed in Fig. 3 for these different types of units. With the bubble size rapidly reaching the saturation value in the 3D units (as indicated by the data in Fig. 4), the same solids ejection velocities will result in similar splash zones, regardless of the dense bed height. However, in the case of the pseudo-2D unit, the larger erupting bubbles in taller beds will yield a higher solids ejection velocity and, thus, a slower solids back-mixing (lower a-value). Further, as seen in Fig. 4, for a dense bed height

Fig. 5. Values of the decay coefficient (modeled by Eq. (7), experimental [5] and correlated through Eq. (4) [5]) as a function of the relative gas velocity, for a) Chalmers boiler and b) fluid-dynamically scaled model of a > 200-MW$_{th}$ CFB boiler.
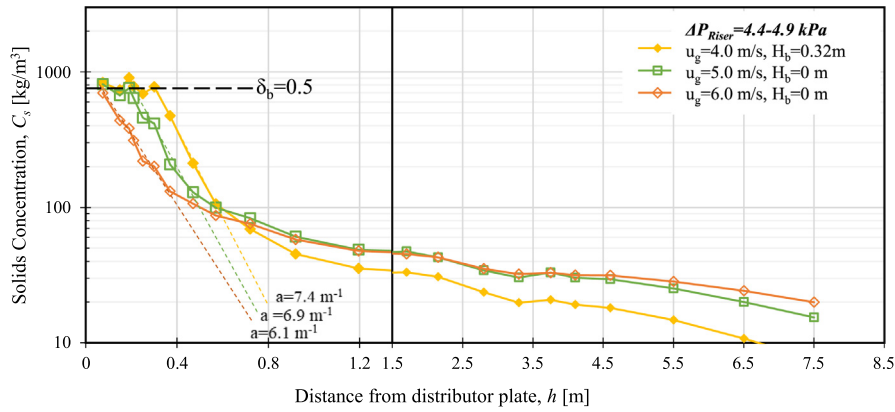
Fig. 6. Vertical profiles of the solids concentration in the pseudo-2D cold unit. Note the different scale on the abscissa at heights <1.5 m above the gas distributor. Three cases with constant riser pressure drop and different fluidization velocity are shown, one yielding the establishment of a dense bed and two not.

the Chalmers boiler data. Regarding the data from scaled experiments resembling a hot, utility-scale unit, the model provides a more accurate prediction than the empirical correlation. In summary, comparing exclusively to validation data (i.e., not used in the fitting), the model based on ballistic trajectories yields an average error of 46% and an empirical correlation of 73%.

As a final remark regarding the solids back-mixing in the bottom region, the authors observed in the cold units used in this work that ejection and splashing of particle clusters still occurred despite the absence of a dense bed. Fig. 6 shows the vertical profiles of the solids concentration at the bottom of the pseudo-2D unit for three different fluidization velocities, of which one (the lowest) yields a dense bed while the higher two do not. It should be noted that different scales are used on the x-axis for better readability. As shown in Fig. 6, a "*splash zone*" (i.e., a region where the exponential decay in solids concentration with height is strong: above 1 m^{-1}) is established in the bottom region for all cases and indicated by the colored frames. Above the "*splash zones*", the transport zones are characterized by a weaker exponential decay in solids concentration (with a decay coefficient well below 1 m^{-1}). Note that the "*splash zones*" corresponding to the cases without a dense bed have a smaller vertical extension than those that originate from a dense bed, despite the higher fluidization velocities.

The "*splash zone*" observed in the absence of a dense bed obviously cannot have arisen as a result of solids ejection from bubble eruptions.

We suggest that the ejection of solids clusters originates instead at the gas distributor (the injection holes or nozzles) where a gas flow which is still strongly fluctuating and heterogeneously distributed, produces an effect similar to that of erupting bubbles in the presence of a bottom bed, i.e., intermittent and locally high gas velocities that are able to eject solids strands. The absence of a dense bed is a well-known phenomenon in narrow CFB units, see e.g. Li (1994), but has only recently been confirmed that can also apply to large-scale CFB boilers [46], and the establishment of this "*splash zone*" in the absence of a bottom bed under conditions representative of large-scale CFB boilers has not been reported previously in the literature. It demonstrates the need for more
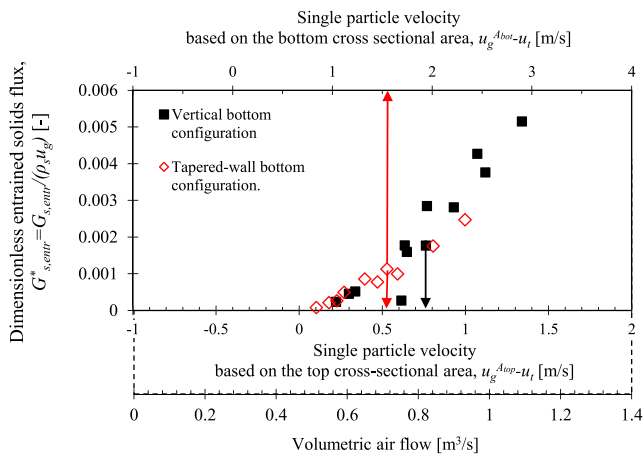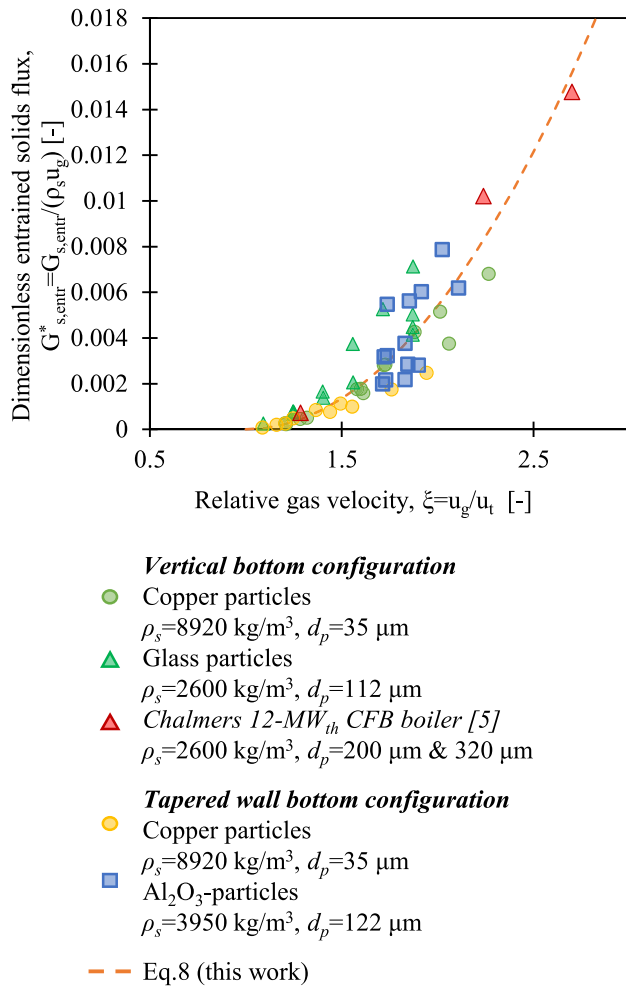

Fig. 7. Dimensionless entrained solids flux from the bottom region, Eq. (6), in different bottom sidewalls configurations (with/without tapered walls) as a function of the single-particle transport velocity in the upper furnace. The upper x-axis provides the single-particle transport velocity at the furnace bottom for the tapered wall cases.
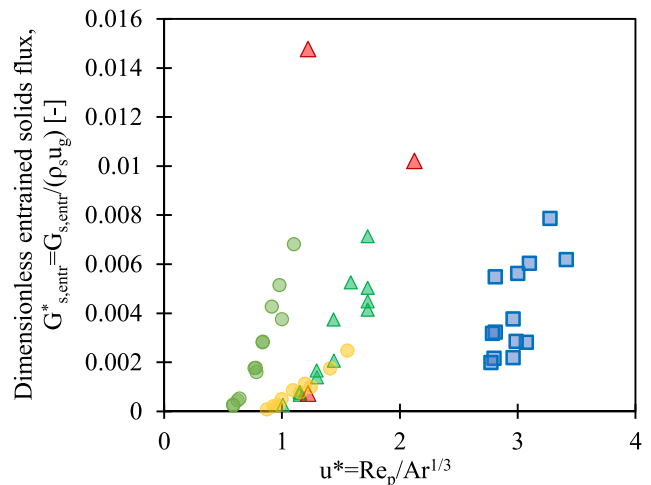
Fig. 8. Dimensionless entrained solids flux from the bottom region as a function of the dimensionless velocity, for different experimental set-ups and particle types.

Fig. 9. Dimensionless entrained solids flux from the bottom region of the furnace as a function of the relative gas velocity. Experimental values (markers) are compared to the correlation proposed in this work in Eq. (8) (dashed line).

generic investigations aimed at uncovering the mechanism/s that create the splash zones in these types of units.

4.2. Entrainment of solids from the splash zone into the transport zone

The flow of solids that is not back-mixed in the splash zone and, therefore, is entrained by the gas into the transport zone [see Eqs. (1) and (5)] is analyzed below. For simplicity, the present analysis is limited to cases in which a dense bed is present (in this way, there is no influence of a non-saturated solids flow at the bottom region when the dense bed is lost; see [18]). Only the data from 3-D units, i.e., not those from the pseudo-2D unit, are considered.

Initially, the influence of tapered-wall geometries on the solids entrainment from the bottom region is studied by modification of the bottom riser configuration in fluid-dynamically down-scaled runs (the riser's front and rear walls were inclined so that the cross-section at the gas distributor level was reduced by 40% compared to that at upper locations). The scaled bed material used mimics hot operation (850 °C) with silica sand as the bed material. Fig. 7 shows the dimensionless fluxes of solids entrained [Eqs. (5) and (6)] from the bottom region measured in the vertical (non-tapered wall configuration) and tapered-wall configurations, respectively. The results indicate that a given air flow (and thus a given value of u_g-u_t at the upper riser, used as bottom x-axis in the figure) in both configurations yields the same

dimensionless flux of solids entrainment. Thus, for a given gas flow the presence of tapered walls does not affect the solids entrainment, despite the higher value of u_g-u_t at the gas distributor level (top x-axis) in the case of tapered walls.

With tapered walls shown to have no effect on the solids entrainment, in contrast to the vertical bottom configuration for a given air flow, measurements of the entrained solids flux are executed in the 3D cold unit, with and without tapered walls, and with different materials (according to Tables.

Table 1 and Table 2). These measurements are complemented with data from earlier measurements made in the 12-MW$_{th}$ Chalmers CFB unit [5] (which has a no-tapered configuration). In summary, the set of experimental data covers a range of dimensionless particles size of $d_p^* = Ar^{1/3} \in [3, 6.3]$ and, as shown in Fig. 8, a range of dimensionless fluidization velocities of $u^* = Re_p/Ar^{1/3} \in [0.6, 3.4]$, yielding dimensionless entrainment flux values [see Eq. (6)] up to approximately 0.015.

With the data shown in Fig. 8, the correlation for the solids entrainment is formulated as a function of the relative gas velocity, $\xi = u_g/u_t$. The expression obtained from the fitting of all the experimental data-points in Fig. 8 reads as follows:

$$G_{s.entr}^* = 0.0054 \, (\xi - 1)^2 \tag{8}$$

Fig. 9 plots this expression together with the experimentally derived values of the dimensionless entrained solids flux. The average error against the measured values is 28%, which is considered highly satisfactory, bearing in mind the wide spectrum of unit sizes, temperature levels, bottom geometries, and particle sizes and densities.

5. Conclusion

The solids back-mixing in the splash zone of large-scale hot units is found to be independent of the dense bed height when typical ranges of the latter are tested. This contrasts with the observations made in cold units. This can be explained by the attainment of a maximum bubble size for typical bed heights, as suggested by measurements made under hot conditions but observed in cold units only at much greater bed heights.

The solids back-mixing in the splash zone can be estimated using a simple model that considers the ballistic trajectories of the solids ejected. Solids concentration profiles modeled on this basis show a somewhat exponential decay, with decay coefficients similar to those measured in hot large-scale units, and showing better agreement with the validation data than the empirical correlation earlier proposed in the literature.

A fluid-dynamic region with similar characteristics as the splash zone is present even in the absence of a dense bottom bed. This zone, in similarity to the splash zone formed in the presence of a dense bed, is a consequence of the local and intermittent occurrences of very high gas velocities. These velocities appear at the gas distributor holes/nozzles in the absence of a dense bed, or at the locations of bubble eruptions in the presence of a dense bed.

The solids entrainment from the bottom region into the transport zone is not affected by the tapered wall configuration. An empirical expression for the solids entrainment (in dimensionless terms) is proposed that describes with an average error of 28% the experimental data obtained for variations in the solids properties, unit geometries, unit sizes, and temperature levels.

Author statement

Tove Djerf: Data Curation; Investigation; Methodology; Writing.
David Pallarès: Methodology; Writing; Supervision.
Filip Johnsson: Writing; Supervision.

Declaration of Competing Interest

The authors declare that they have no known competing financial interests or personal relationships that could have appeared to influence the work reported in this paper.

Acknowledgments

References

[1] B. Leckner, L. Thorson, J. Kjärstad, F. Johnsson, Utilization of fluidized bed boilers – a worldwide overview, Developments in Fluidized Bed Conversion 2011 to 2016. 2016, IEA-FBC TCP: Presented at IEA-FBC 73rd Technical Meeting, Tokyo, Japan, December 2016.

[2] B. Leckner, Developments in fluidized bed conversion of solid fuels, Therm. Sci. 20 (Suppl. 1) (2016) 1–18.

[3] J. Koornneef, M. Junginger, A. Faaij, Development of fluidized bed combustion—an overview of trends, performance and cost, Prog. Energy Combust. Sci. 33 (1) (2007) 19–55.

[4] IEA, in: I.E. Agency (Ed.), Energy, Climate Change and Environment 2016 Insights, 2016 , Paris, France.

[5] F. Johnsson, B. Leckner, Vertical distribution of solids in a CFB-furnace, CONF-950522, American Society of Mechanical Engineers, New York, NY (United States), 1995.

[6] A. Svensson, F. Johnsson, B. Leckner, Bottom bed regimes in a circulating fluidized bed boiler, Int. J. Multiphase Flow 22 (6) (1996) 1187–1204.

[7] A. Svensson, F. Johnsson, B. Leckner, Fluidization regimes in non-slugging fluidized beds: the influence of pressure drop across the air distributor, Powder Technol. 86 (3) (1996) 299–312.

[8] L. Glicksman, M. Hyre, P. Farrell, Dynamic similarity in fluidization, Int. J. Multiphase Flow 20 (1994) 331–386.

[9] P. Markström, A. Lyngfelt, Designing and operating a cold-flow model of a 100 kW chemical-looping combustor, Powder Technol. 222 (2012) 182–192.

[10] G. Schöny, E. Zehetner, J. Fuchs, T. Pröll, G. Sprachmann, H. Hofbauer, Design of a bench scale unit for continuous CO2 capture via temperature swing adsorption—fluid-dynamic feasibility study, Chemical Engineering Research Design 106 (2016) 155–167.

[11] S. Sasic, F. Johnsson, B. Leckner, Interaction between a fluidized bed and its air-supply system: some observations, Ind. Eng. Chem. Res. 43 (18) (2004) 5730–5737.

[12] E. Sette, D. Pallarès, F. Johnsson, Experimental quantification of lateral mixing of fuels in fluid-dynamically down-scaled bubbling fluidized beds, Appl. Energy 136 (2014) 671–681.

[13] B. Leckner, P. Szentannai, F. Winter, Scale-up of fluidized-bed combustion–a review, Fuel 90 (10) (2011) 2951–2964.

[14] D. Pallares, F. Johnsson, Macroscopic modelling of fluid dynamics in large-scale circulating fluidized beds, Prog. Energy Combust. Sci. 32 (5–6) (2006) 539–569.

[15] W. Zhang, F. Johnsson, B. Leckner, Fluid-dynamic boundary layers in CFB boilers, Chem. Eng. Sci. 50 (2) (1995) 201–210.

[16] A. Johansson, F. Johnsson, B. Leckner, Solids back-mixing in CFB boilers, Chem. Eng. Sci. 62 (1–2) (2007) 561–573.

[17] J.C. Schouten, R.C. Zijerveld, C.M. van den Bleek, Scale-up of bottom-bed dynamics and axial solids-distribution in circulating fluidized beds of Geldart-B particles, Chem. Eng. Sci. 54 (13–14) (1999) 2103–2112.

[18] T. Djerf, D. Pallarès, F. Johnsson, Solids flow patterns in large-scale circulating fluidised bed boilers: experimental evaluation under fluid-dynamically down-scaled conditions, Chem. Eng. Sci. 231 (2020) 1–16.

[19] T. Djerf, D. Pallarès, F. Johnsson, Bottom-bed fluid dynamics–influence on solids entrainment, Fuel Process. Technol. 173 (2018) 112–118.

[20] A. Gómez-Barea, B. Leckner, Modeling of biomass gasification in fluidized bed, Progress in Energy Combustion Science 36 (4) (2010) 444–509.

[21] F. Johnsson, S. Andersson, B. Leckner, Expansion of a freely bubbling fluidized bed, Powder Technol. 68 (2) (1991) 117–123.

[22] T. Karlsson, X. Liu, D. Pallarès, F. Johnsson, Solids circulation in circulating fluidized beds with low riser aspect ratio and varying total solids inventory, Powder Technol. 316 (2017) 670–676.

[23] H. Do, J. Grace, R. Clift, Particle ejection and entrainment from fluidised beds, Powder Technol. 6 (4) (1972) 195–200.

[24] A.S. Fung, F. Hamdullahpur, A gas and particle flow model in the freeboard of a fluidized bed based on bubble coalescence, Powder Technol. 74 (2) (1993) 121–133.

[25] F. Johnsson, A. Svensson, S. Andersson, B. Leckner, Fluidization Regimes in Boilers, Fluidization VIII. 1995, International Symposium of the Engineering Foundation: Tours, France 1995, pp. 129–136.

[26] B. Leckner, Regimes of large-scale fluidized beds for solid fuel conversion, Powder Technol. 308 (2017) 362–367.

[27] D. Pallarès, F. Johnsson, Modeling of fluidized bed combustion processes, in: F. Scala (Ed.), Fluidized Bed Technologies for Near-Zero Emission Combustion and Gasification, Woodhead Publishing Series in Energy, Italy 2013, pp. 524–578.

[28] J. Wang, Z. Sun, Y. Shao, J. Zhu, Operating regimes in circulating fluidized bed combustors: fast fluidization or bubbling-entrained bed? Fuel 297 (2021) , 120727.

[29] D. Santana, S. Nauri, A. Acosta, N. García, A. Macías-Machín, Initial particle velocity spatial distribution from 2-D erupting bubbles in fluidized beds, J Powder Technology 150 (1) (2005) 1–8.

[30] R. Darton, R. LaNauze, J. Davidson, D. Harrion, Bubble-growth due to coalescene in fluidised beds, Trans. Inst. Chem. Eng. 55 (1977).

[31] J. Davidson, D. Harrison, J.R. Guedes de Carvalho, Liquidlike behavior of fluidized beds, Annu. Rev. Fluid Mech. 9 (1977).

[32] F. Scala, Fluidized Bed Technologies for Near-Zero Emission Combustion and Gasification, Elsevier, 2013.

[33] A. Ajbar, K. Alhumaizi, A. Ibrahim, M. Asif, Hydrodynamics of gas fluidized beds with mixture of group D and B particles, Can. J. Chem. Eng. 80 (2) (2002) 281–288.

[34] C. Daw, J. Halow, Evaluation of control of fluidization quality through chaotic time series analysis of pressure-drop measurements, AIChE. Symposium, Oak Ridge National Lab, TN (United States), 1992.

[35] D. Kunii, O. Levenspiel, Fluidization Engineering, 1991.

[36] C. Wen, L. Chen, Fluidized bed freeboard phenomena: entrainment and elutriation, AICHE J. 28 (1) (1982) 117–128.

[37] D. Kunii, O. Levenspiel, Entrainment of solids from fluidized beds I. Hold-up of solids in the freeboard II. Operation of fast fluidized beds, Powder Technol. 61 (2) (1990) 193–206.

[38] Z. Man, B. Rushan, Y. Zezhong, J. Xiaoguo, Heat flux profile of the furnace wall of a 300 MWe CFB boiler, Powder Technol. 203 (3) (2010) 548–554.

[39] H. Yang, H. Zhang, S. Yang, G. Yue, J. Su, Z. Fu, Effect of bed pressure drop on performance of a CFB boiler, Energy Fuel 23 (6) (2009) 2886–2890.

[40] H. Yang, G. Yue, X. Xiao, J. Lu, Q. Liu, 1D modeling on the material balance in CFB boiler, Chem. Eng. Sci. 60 (20) (2005) 5603–5611.

[41] J.H. Choi, J.E. Son, S.D. Kim, Solid entrainment in fluidized bed combustors, J. Chem. Eng. Jpn. 22 (6) (1989) 597–606.

[42] D. Merrick, J. Highley, Particle size reduction and elutriation in a fluidized bed process, AIChE Symp, 1974.

[43] L.R. Glicksman, Scaling relationships for fluidized beds, Chem. Eng. Sci. 39 (9) (1984) 1373–1379.

[44] B. Leckner, Boundary layers-first measurements in the 12 MW CFB research plant at Charmers University, Proc. 11th Int. Conf. on Fluidized Bed Combustion, Montreal, Canada, 1991, ASME, 1991.

[45] E. Peirano, V. Delloume, B. Leckner, Two-or three-dimensional simulations of turbulent gas–solid flows applied to fluidization, Chem. Eng. Sci. 56 (16) (2001) 4787–4799.

[46] Y. Li, Hydrodynamics, Advances in Chemical Engineering, Elsevier 1994, pp. 85–146.